



Co-published by  
**Institute of Fluid-Flow Machinery**  
Polish Academy of Sciences  
**Committee on Thermodynamics and Combustion**  
Polish Academy of Sciences

Copyright©2024 by the Authors under license CC BY 4.0

<http://www.imp.gda.pl/archives-of-thermodynamics/>



## Allometry of nanoparticles in diesel-biodiesel blends for CI engine performance, combustion and emissions

Mohd Mujtaba Ahmed<sup>a\*</sup>, Harveer Singh Pali<sup>a</sup>, Mohammad Mohsin Khan<sup>a</sup>

<sup>a</sup> Department of Mechanical Engineering, National Institute of Technology Srinagar, J&K 190006 India

\* Corresponding author email: mohdmujtabaahmed5@gmail.com

Received: 08.07.2023; revised: 02.11.2023; accepted: 04.01.2024

### Abstract

Most countries in the world are facing two major challenges, one is the increase in the demand for energy consumption difficult to fulfill because of limited fossil fuel, and the second is the emission norms specified by many countries. Various methods are adopted to reduce emissions from engines but that leads to sacrificing the performance of CI engines. To eradicate this problem in the present study, the nanoparticles like (TiO<sub>2</sub>) are used with different particle sizes 10–30 nm, 30–50 nm and 50–70 nm induced in B20 (20% biodiesel and 80% diesel) with the constant volume fraction of 100 ppm, and utilized in the diesel engine without any modifications. The results showed that the incorporation of TiO<sub>2</sub> nanoparticles improves the combustion of hydrocarbons and reduces the emissions of CO, unburned hydrocarbon concentration, NO<sub>x</sub> and soot. Moreover, among three sizes of the nanoparticles, those with size 30–50 nm showed interesting results with the reduction in brake-specific energy consumption, NO<sub>x</sub>, smoke and HC by 2.9%, 16.2%, 35% and 10%, respectively, compared to other blends used in the study, and hence the blend with the nanoparticle of size 30–50 nm is expected to be a more promising fuel for commercial application in CI engines.

**Keywords:** Biodiesel; Nanoparticle; CI engine; Engine performance; Engine combustion; Exhaust emission.

Vol. 45(2024), No. 1, 99–108; doi: 10.24425/ather.2024.150442

Cite this manuscript as: Ahmed, M.M., Pali, H.S., & Khan, M.M. (2024). Allometry of nanoparticles in diesel-biodiesel blends for CI engine performance, combustion and emissions. *Archives of Thermodynamics*, 45(1), 99–108.

### 1. Introduction

Due in part to their great thermal efficiency and high reliability, diesel-fuelled engines are frequently used as prime movers in the transportation and industrial sectors. Diesel engine reliance has grown, resulting in higher fossil fuel usage [1]. On the other hand, heavy-duty vehicles that run on traditional fuels like diesel are the biggest producers of greenhouse gas emissions [2]. Using sustainable alternatives like biofuels in place of fossil fuels can help cut down on carbon emissions [3].

For the production of biodiesel, raw resources such as vegetable oil and animal fat are used. The materials used to produce biodiesel undergo transesterification as this is a commonly used method for biodiesel production [4, 5], which restructures their molecules and makes them acceptable as a replacement for diesel engines [6–8]. There are also drawbacks to neat biodiesel, including higher emissions of NO<sub>x</sub>, limited energy yield, and high specific fuel consumption [9]. By fulfilling particular fuel criteria, the use of additives has demonstrated its ability to get beyond these restrictions [3, 10, 11]. Microscale-sized additions show a slight reduction in emissions; however, studies show that

## Nomenclature

### Abbreviations and Acronyms

ASTM	– American Society of Testing Materials
bTDC	– before top dead center
B20N30	– 20% biodiesel + 80% diesel + 100 ppm TiO <sub>2</sub> (10–30 nm)
B20N50	– 20% biodiesel + 80% diesel + 100 ppm TiO <sub>2</sub> (30–50 nm)
B20N70	– 20% biodiesel + 80% diesel + 100 ppm TiO <sub>2</sub> (50–70 nm)
BP	– brake power
BSEC	– brake specific energy consumption
BSFC	– brake specific fuel consumption
BTE	– brake thermal efficiency
CA	– crank angle

CHRR	– cumulative heat release rate
CI	– compression ignition
CPP	– cylinder peak pressure
HRR	– heat release rate
NO <sub>x</sub>	– oxides of nitrogen
UHC	– unburned hydrocarbons
VCR	– variable compression ratio
WCO	– waste cooking oil
XHC	– amount of unburned hydrocarbons
XCO	– amount of carbon monoxide
XNO <sub>x</sub>	– amount of oxides of nitrogen

the use of big additive particles may negatively impact combustion performance, increasing emissions and decreasing efficiency [12–14]. The higher density of the droplets holding additives, which makes it challenging to have a homogeneous combination of fuels and additives, could be the cause of this phenomenon. Additionally, this can cause the droplets holding the addition to settle, resulting in sedimentation. Another drawback is that larger particles require longer times to complete physical and chemical processes when combined with base fuel, increasing ignition delay. Increased exhaust emissions and incomplete combustion are caused by a longer delay period. Thus, the use of large-sized additives in biodiesel blends is embarrassed by these criteria.

However, by adding nanosized metal oxide particles (100 nm) to biodiesel blends, these restrictions can be bypassed. They have distinct advantages to micro-sized additives, including a larger surface-to-volume ratio, stronger thermal conductivity, and superior lubricating qualities [15]. A nanofluid is created when nano-particles are combined with a base, like water, fuel, biofuels, etc. The nanofluid has various advantages over the base fluid, including better lubricity and increased thermal conductivity. The effective transport of heat, which is crucial during engine combustion, is made possible by these qualities. Additionally, nanoparticles with relatively tiny diameters prevent sedimentation by improving their dispersion and causing more chaotic movements. Owing to the nanofluid advanced thermal conductivity, which was described earlier, when it is injected into the combustion chamber through the fuel injector, there may be a greater heat exchange between the biodiesel and air. Compared to the combustion of plain fuel, this immediately primes the air-fuel mixture for spontaneous combustion, shortening the ignition delay. So, with lesser emissions, improved combustion and engine performance can be attained.

Experimental research has been done on biodiesel compositions using nanoparticle additions to power diesel engines. Jia-qiang et al. [16] investigated how nanoparticle size affected the diffusion stability of alumina (13 and 28 nm) added to biodiesel made from jatropha. The 13 nm nano-particles with a 0.1 volume percentage were said to have unchanged stability for more than a year. Kumar et al. [17] studied how ferric nanoparticles affected the characteristics of a biodiesel-powered diesel engine. The research noticed an increased brake thermal efficiency (BTE), reduced fuel consumption, and decrement in the amount of carbon monoxide (XCO) and hydrocarbon (XHC) after add-

ing 1 percent in volume of ferrofluid nano-additive to B20. Prabu et al. [18] used alumina (Al<sub>2</sub>O<sub>3</sub>) and cerium (CeO<sub>2</sub>) nanoparticles to experimentally study the performance parameters of a traditional diesel-fuelled engine. They noted that the addition of nanoparticles often reduced the delay and expedited early combustion start and that Al<sub>2</sub>O<sub>3</sub> as a nano additive produced a greater BTE than nanoceria.

Ramesh et al. [19] studied the impact of diffusing alumina nanoparticles to biodiesel made from chicken litter on an engine performance, emissions, and combustion style. They claimed that alumina nanoparticle-added biodiesel had a higher BTE than plain biodiesel fuel. Silva et al. [20] examined the impact of Pongamia biodiesel (B20) containing TiO<sub>2</sub> nano-particles on diesel engine combustion. With the exception of nitrogen oxides, the fuels that were combined with nanoparticles burned more efficiently and produced significantly fewer pollutants (NO<sub>x</sub>). The fuel mixture with 75 ppm of nanoparticles, according to the authors, showed the most encouraging results. Kao et al. [21] made combustion tests employing fuels containing an aqueous aluminium nanofluid in a diesel engine. They saw an increase in the burning rate when the aqueous aluminium nanofluid was present. Similarly, Xin et al. [22] hypothesized that adding nanoceria as a nano additive increased combustion efficiency, probably as a result of the increased pressure and lengthened burning time.

The extreme possible cylinder-pressure of nano-particles mixed fuel was also observed to be greater than that for neat conventional diesel, and nanoparticle-blended fuels were linked to shorter igniting delays than traditional diesel fuel [22]. Kumar et al. [23] examined the effects of injection pressure and nano CeO<sub>2</sub> (80 ppm) on a biodiesel-powered diesel engine thermal behaviour (B20). At the greatest injection pressure of 240 bar, the cerium oxide nanoparticle-doped fuel showed improved performance with decreased emissions [15, 23].

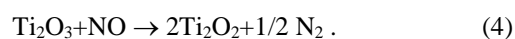
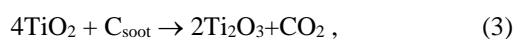
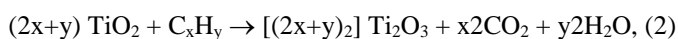
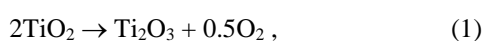
Sajith et al. [24] studied experimentally the effects of nanoceria as a fuel-additive in Jatropha biodiesel. According to their findings, utilizing plain biodiesel had a lower BTE at full load than using nanoparticle-dispersed biofuel. Additionally, the fuel formulation treated with CeO<sub>2</sub> nanoparticles showed decreased NO<sub>x</sub> concentrations (XNO<sub>x</sub>). Additionally, Mirzajanzadeh et al. [25] claimed that burning fuel that contained cerium oxide nanoparticles (40–50 nm in size) and waste cooking oil (WCO) significantly reduced NO<sub>x</sub> emissions. The biggest reduction in XNO<sub>x</sub> was 18.9% for the highest concentration of CeO<sub>2</sub>

nanoparticles utilized by the authors, which was 90 ppm. This research used many variable concentrations of the nano additives, including 30, 60, and 90 ppm. Selvan et al. [26] reported that running the tested diesel engine on fuel formulations including CeO<sub>2</sub> nanoparticles resulted in a 54% reduction in XNO<sub>x</sub>.

The type of biodiesel and the various characteristics of the nanoparticles used as an additive could have a significant impact on how well an engine performs when using diesel and biodiesel fuel mixes with nano additives (kind, magnitude, morphology, oxide layer width and volume fraction). Numerous studies have been conducted to determine the impacts of several biodiesel kinds and various volume concentrations of nanoparticles. The effect of nanoparticle size on engine performance and emission characteristics, however, is little understood. This study, which examines the performance, combustion and emission characteristics of a diesel engine running on a blend of biodiesel (WCO) and diesel fuel (B20), which contains TiO<sub>2</sub> nanoparticles of various sizes (10–30 nm, 30–50 nm and 50–70 nm), intends to fill this knowledge gap as a result. Measurements and analyses were made for performance factors, such as brake thermal efficiency (BTE), brake-specific energy consumption (BSEC), cylinder peak pressure (CPP), and heat release rate (HRR), as well as engine tailpipe emissions, such as XCO, XHC, XNO<sub>x</sub>, and smoke opacity.

### 1.1. Background of TiO<sub>2</sub> nanoparticle as a combustion catalyst in diesel engines

TiO<sub>2</sub> is an indispensable component of biodiesel thanks to the high proportion of oxidation it contains. TiO<sub>2</sub> nanoparticles are extensively utilized in the production of a variety of products, such as paints, plastics, textiles, cosmetics, and coatings. Around the world, millions of metric tonnes of TiO<sub>2</sub> are produced in manufacturing facilities each year. One of the benefits of using TiO<sub>2</sub> is that it has a high dispersion quality. The addition of the nanoparticle to the biodiesel does not result in a change in the viscosity of the fuel, in contrast to the addition of pentanol and other additives. There aren't many pieces of research that back up the claim that vegetable oil and organic solvents can achieve a 99% dispersion rate. In addition to this, their thermal qualities are significantly enhanced, and they have the ability to resist corrosion. These TiO<sub>2</sub> nanoparticles are produced by a process known as sol-gel fabrication. Figure 1 shows the physical appearance and specifications of TiO<sub>2</sub> nanoparticles incorporated into the B20 fuel blend. When the temperature in the combustion chamber rises, the TiO<sub>2</sub> nanoparticle discharges its oxygen molecule, which increases the rate of combustion, resulting in proper combustion and hence reducing emissions at the exhaust. The following equations illustrate the reactions occurring during the combustion process:



Specifications	Volumes
Purity (%)	99.9
Colour	White solid
Titanium content (%)	58.36
Oxygen content (%)	41.05
Solubility nature	Insoluble in water
Molecular weight (gm/mol)	79.87
Density (gm/cm <sup>3</sup> )	4.29
Boiling point (°C)	2972
Melting point (°C)	1843

Fig. 1. Physical appearance and specifications of TiO<sub>2</sub> nanoparticle.

## 2. Materials and methods

### 2.1. Fuel Blend Preparation

Biodiesel from waste cooking oil (WCO) collected from the local mess and restaurants has been produced from the process of transesterification in the laboratory with similar conditions adopted by the previous experiment [27], and its physicochemical properties have been evaluated with ASTM standards with B20 (80% diesel and 20% biodiesel) which is itemized in Table 1. Various dimensions of Titanium oxide nanoparticles (i.e., 10–30 nm, 30–50 nm, and 50–70 nm) have been used in the preparation of test fuels. Table 2 shows the nomenclature of the samples used in the study. The produced fuels were designated as B20N30, B20N50 and B20N70. The two-step process in which magnetic stirring followed by ultrasonication was used to blend the nanoparticles and B20 fuel to form a homogenous mixture with a good distribution of TiO<sub>2</sub> nanoparticles in the test fuel. Figure 2 depicts the physical appearance of produced test fuels. All the test samples, after two-step physical stabilization, were used immediately in the engine.

Table 1. Tested values obtained for physicochemical properties of B20 blend.

Physicochemical Properties	B100	B20	Diesel	ASTM Standards
Higher heating value (MJ/kg)	37.9	40.23	43.2	D240
Flash point (°C)	370	67	321	D93
Density kg/m <sup>3</sup>	877	852	820	D4052
Kinematic viscosity (cSt)	4.5	3.8	3.4	D445

Table 2. Nomenclature of test sample used in the study.

Nomenclature	Understanding
B20	20% biodiesel +80% diesel
B20N30	20% biodiesel + 80% diesel + 100 ppm TiO <sub>2</sub> (10–30 nm)
B20N50	20% biodiesel + 80% diesel + 100 ppm TiO <sub>2</sub> (30–50 nm)
B20N70	20% biodiesel + 80% diesel + 100 ppm TiO <sub>2</sub> (50–70 nm)



Fig. 2. Physical appearance of test fuel blends.

## 2.2. Test setup and experimentation

The testing of various test fuels was conducted on a single-cylinder variable VCR diesel engine with a hydraulic dynamometer and compression ratio of 16:1. The setup was also integrated with the sensors which measure the fuel flow rate, load, cylinder pressure, the position of crank angle and air flow rate. The engine performance metrics are measured with the help of engine software provided with the setup. The concentration of exhaust gases like CO, HC, NO<sub>x</sub>, O<sub>2</sub> and CO<sub>2</sub> were measured with the help of a multi-gas analyzer. The AVL smoke meter was attached with the setup for recording the emissions data. Table 3 and Table 4 provide the range and resolution of the instruments that are used in the experiment for test execution. Figure 3 shows a schematic illustration of the experimental setup

Table 3: Specifications of setup.

Description	Value/Description
Basic engine	Kirloskar
Make	TECH - ED
Diameter bore (mm)	80
Length of stroke (mm)	110
Compression ratio (CR)	12:1 to 20:1
Speed (constant)	1500 rpm
Rated brake power (kW)	Up to 4
Normal injection pressure (bar)	180
Dynamometer	Hydraulic dynamometer

Table 4. Specifications of gas analyzer and smoke meter.

Item	Range	Resolution
Pressure (bar)	0.344–75	0.0069
HC emissions (ppm)	0–15 000	1
Smoke opacity	0–100	0.01
NO <sub>x</sub> emissions (ppm)	0–5 000	1
CO <sub>2</sub> emissions (vol %)	0–20	0.01
O <sub>2</sub> emissions (vol %)	0–25	0.1
CO emissions (vol %)	0–9.99	0.001

## 2.3. Uncertainty analysis

Uncertainty analysis in laboratory experiments examines how uncertain any measurements are. It enables the estimation of a physical variable's numerical value and the impact of instrumentation faults on that value. Equation 5 was used in this study to compute the uncertainty of a depending variable utilizing measurement errors for parameters which are independent like

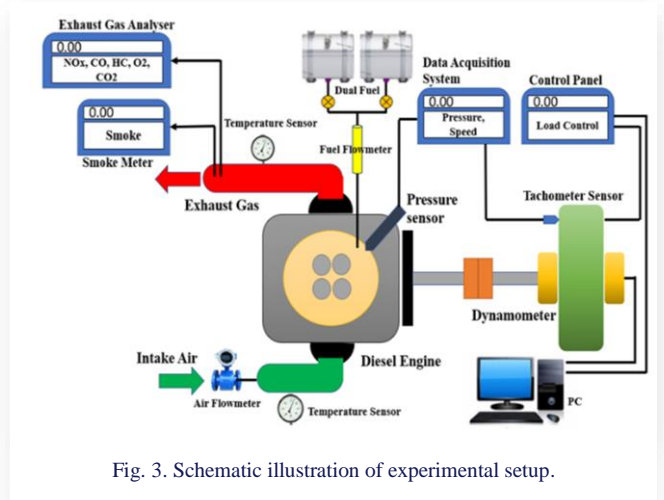


Fig. 3. Schematic illustration of experimental setup.

load, speed and fuel flow rate. Table 5 lists the determined uncertainty values for several constraints.

$$W_R = ([(\partial R/\partial X_1) w_1]^2 + [(\partial R/\partial X_2) w_2]^2 + \dots + [(\partial R/\partial X_n) w_n]^2)^{1/2}. \quad (5)$$

Table 5. Percentage uncertainty values of some parameters in the study.

Quantity	Uncertainty (%)
Load	0.64
Speed	0.55
Flow rate of fuel	0.9
BSEC	1.8
Concentration of NO <sub>x</sub>	2.1
Concentration of HC	2.3
Concentration of CO	1.8
Smoke	0.98

## 3. Results and discussion

### 3.1. Brake thermal efficiency

BTE describes the effective transformation of energy present in the injected fuel into valuable work. Figure 4 illustrates the effects of various test fuels on BTE of the setup for different loads, and it is detected that BTE increases with the increment in engine load [28]. The engine is equipped with the software which calculates the BTE on the basis of Eq. (6). When the engine is fuelled with biodiesel and its blends, a slight decrement in the BTE has been observed. The credit for this reduction falls on the biodiesel's lower calorific value, which lowers the cumulative

energy of the test fuel blend [29, 30]. The examination also revealed that the incorporation of TiO<sub>2</sub> nanoparticles of various sizes enhances the brake thermal efficiency of the engine [31]. Moreover, among the three sizes of TiO<sub>2</sub> nanoparticles, the optimum values of BTE are noted for the blend containing the nanoparticles of size 30–50 nm size as compared to those of 10–30 nm and 50–70 nm. The causes for this enhancement are fuel oxidation leading to proper combustion, high surface-to-volume ratio and improved catalytic activity because of smaller size nanoparticles (30–50 nm). Further, smaller size (10–30 nm) particles also diminish the fuel properties, as they may not improve the density and viscosity of the test fuel blends. The BTE increments for the blend B20N50, as compared to B20N30 and B20N70, are 3.42% and 6.45% at full load.

$$BTE = \frac{\text{Brake power}}{\text{Heat released}} = \frac{\text{Brake power}}{\text{mass of fuel consumed} \times \text{calorific value}} \quad (6)$$

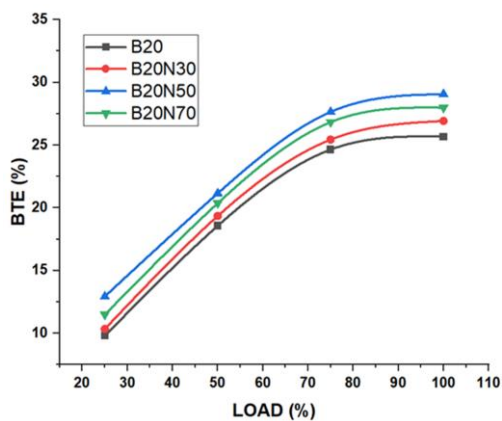


Fig. 4. Variations of brake thermal efficiency for various fuel blends with respect to load.

### 3.2. Brake specific energy consumption

Generally, brake specific energy consumption (BSEC) shows the consumption of energy per unit, which is the specific output of the engine (BP). This is higher when the load is low and becomes reduced when the load is increased up to 80% of the full load of the engine [32]. The illustrated data in Fig. 5 reflects that among all the test blends of nano additives doped fuel blends, that with the nanoparticle size of 30–50 nm shows the lowest BSEC. The B20 blend had superior fuel preparation when TiO<sub>2</sub> nano additives were added, which improved the heat flow between the air and fuel droplets. This must have aided in improving combustion and reducing ignition delay. Due to the efficient use of the injected fuel, these factors probably helped lower BSEC. According to the findings of the current investigation, energy consumption appears to be significantly influenced by particle sizes. B20 + (30–50) nm (B20N50) and B20 + (50–70) nm (B20N70) were at the extremities of the tested fuel formulation, with the former revealing the smallest BSEC and the latter the lowest BSEC. One might draw the generalization that energy combustion declined as nanoparticle size increased. As was previously said, smaller particle sizes result in an increase in the surface-to-volume ratio, helping to achieve

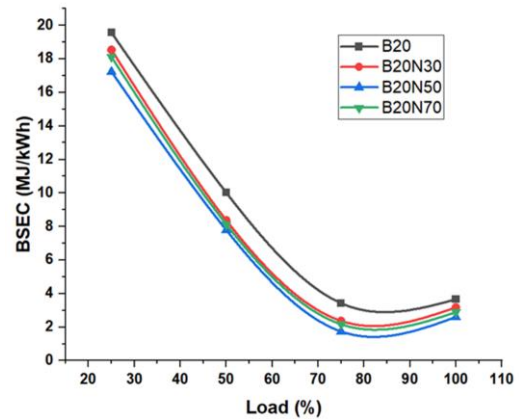


Fig. 5. Variations of brake specific energy consumption for various fuel blends with respect to load.

consistent air-fuel mixing. This accelerates heat transport, shortening the ignition delay. A shorter ignition delay enhances combustion and lowers BSEC.

In the current investigation, a nanoparticle size of 30–50 nm (B20N50) was shown to have the lowest BSEC. Due to the lesser density, a nanoparticle that was too small could not have been able to travel to different areas of the combustion chamber effectively, leading to uneven fusing. This probably lengthened the ignition delay, resulting in inefficient combustion and a small increase in BSEC as a result.

### 3.3. Cylinder peak pressure

The efficiency of combustion is indicated by the cylinder peak pressure (CPP). A higher cylinder pressure can typically be reached if the fuel mixture completely burns during the pre-mixed phase. Additionally, this leads to higher power production and lower emissions [33]. As per the data in Fig. 6, CPP obtained using fuels fused with TiO<sub>2</sub> nanoparticles was higher than that of B20 without additives.

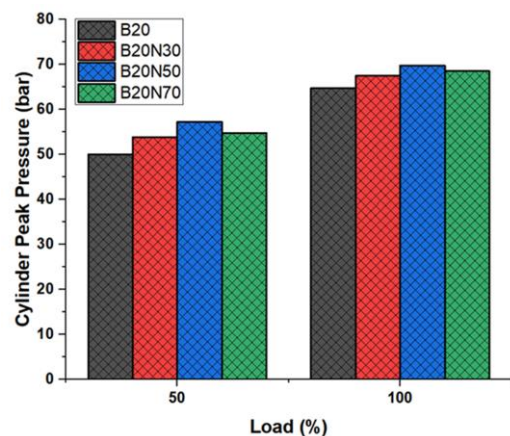


Fig. 6. Variations of cylinder peak pressure for various fuel blends with respect to partial and full load.

TiO<sub>2</sub> nanoparticles must have served as a heat carrier medium when they were added to the B20 fuel mixture, encourag-

ing heat transmission between the fuel drops and air. This phenomenon must have accelerated the fuel droplet evaporation, shortening the delay. As a result, compared to B20 without additives, the autoignition temperature was reached more quickly. These elements helped to provide a higher cylinder peak pressure around the top dead center (TDC) and smooth combustion. The fuel formulation with 30–50 nm nanoparticles had the highest peak of 56.7 bar and 72.3 bar at partial load and full load, respectively, compared to the other two, also this is by 9.35% higher than for B20. As observed in the case of B20 + (50–70) nm (B20N70), less heat transfer occurs when the surface-to-volume ratio drops as the particle size grows. Out of the three fuel variations, B20 fuel had the lowest peak cylinder pressure measurement (see Fig. 6).

### 3.4. Heat release rate

This is the major factor for analysing the combustion process of the engine which shows the heat released per degree crank angle in the cylinder [34]. The heat release rate (HRR) while operating under full load at 26°C CA bTDC is shown in Fig. 7. The phases of combustion are called "premixed combustion", "controlled combustion" and "late combustion", respectively. During the ignition delay period, a negative slope is produced as a result of the cooling effect induced by fuel evaporation. When loaded to its maximum capacity, the B20N30 blend has an HRR of 58.54 J/°CA. Because of their higher viscosity, lower rate of vaporization, larger molecular weight and slower burning velocity, other biodiesel blends have a lower heat release rate.

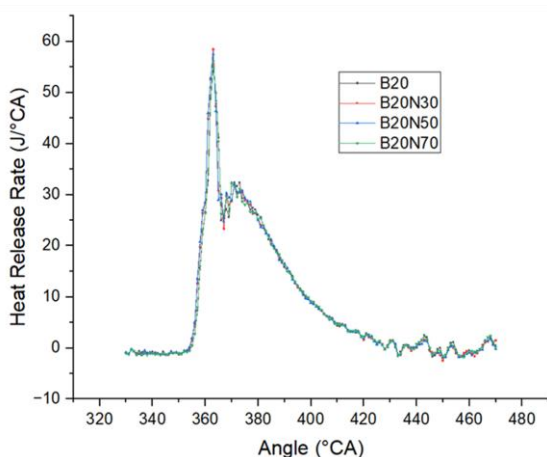


Fig. 7. Variations of heat release rate for various fuel blends with respect to partial and full load.

The blend B20N50 possessed a higher heat release rate comparable to the B20 heat release rate of 54.91 J/°CA. This is because a longer delay between the ignition and combustion led to a higher fuel deposit. When compared to B20, blends with TiO<sub>2</sub> nanoparticles of size 30–50 nm (B20N50) have a superior fuel-air combination, which results in a higher quantity of heat release [35].

### 3.5. Cumulative heat release rate

Figure 8 displays the total heat released for each of the tested fuel blends. The total amount of heat released during the premixed and diffused combustion phases of fuel combustion is shown by these measurements [32, 36]. The beginning and end

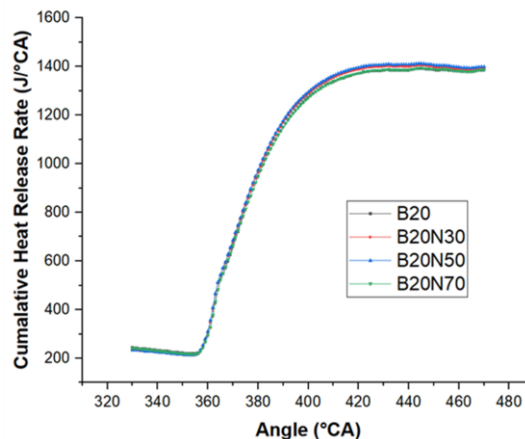


Fig. 8. Variations of cumulative heat release rate for various fuel blends with respect to crank angle.

of combustion, the kind and quality of the fuel, and the rate of pressure rise inside the cylinder are only a few of the variables that affect the total amount of heat released. The addition of TiO<sub>2</sub> nanoparticles worked as a catalyst for the catalytic oxidation of CO and UHC to CO<sub>2</sub>, promoting combustion. Additional energy was released as a result, which would have otherwise remained as unburned fuel in the exhaust.

The power output rose in line with the cumulative heat release during combustion caused by the added energy. B20 + (30–50) nm (B20N50) exhibited the greatest cumulative heat release of 1412.3 J, which is 3.5%, 1.4% and 1.2% higher than the other three test samples B20, B20N30 and B20N70 used in the experiment, respectively.

### 3.6. TiO<sub>2</sub>'s catalytic properties and emission regulation

For a catalyst to be effective in the combustion of diesel engines, it must possess the following three qualities: complete hydrocarbon oxidation, avoiding the creation of nitrogen oxides, and having good thermal stability [37]. TiO<sub>2</sub> can contribute oxygen to the oxidation of soot and hydrocarbons. The fact that a TiO<sub>2</sub> catalyst may donate O<sub>2</sub> for the oxidation reaction and activates at low temperatures (typically 300–500°C) makes it special. High temperatures are required for combustion in diesel engines; the diesel flame typically reaches a temperature of around 1700°C. The chemical interactions between nitrogen and oxygen are likely to produce nitrogen oxides at this high temperature. TiO<sub>2</sub> nanoparticles served as a catalyst and encouraged more thorough combustion of the fuel that was injected. Because nitrogen has a high activation energy, the average cylinder temperature drops during the conversion of NO to N<sub>2</sub>. This also contributes to the reduction of nitrogen oxide production. Additionally, TiO<sub>2</sub> nanoparticles great heat stability promotes their catalytic

activity.  $\text{TiO}_2$  goes through early oxidation after the initial combustion is accomplished. This is due to the thermal stability of nano titanium, which also makes it active after re-oxidation for additional catalytic action. Thus, as demonstrated in Eqs. (2)–(4), the concentrations of CO, HC, and  $\text{NO}_x$  and soot are reduced by oxidation and reduction reactions that occur in  $\text{TiO}_2$  nanoparticles.

$\text{TiO}_2$  catalytic activity is strongly correlated with its surface area. The carbon combustion activation temperature was seen to drop from  $700^\circ\text{C}$  to  $300^\circ\text{C}$  when the surface area of  $\text{TiO}_2$  nanoparticles increased 20 times [38]. The size of the nanoparticle is decreased to produce a larger surface area. When soot and UHC that have adhered to the combustion chamber walls come into touch with the nanoparticles, they oxidize to  $\text{CO}_2$ , reducing tailpipe emissions and enhancing fuel efficiency. Small  $\text{TiO}_2$  nanoparticles are thus preferred since they have a stronger catalytic effect.

### 3.6.1. Unburned hydrocarbon concentration

The fluctuations of unburned hydrocarbon concentration (UBHC) for the various fuel preparations under various engine load levels are shown in Fig. 9. Higher values were seen at full load when HC grew along with the load. The level of HC emissions was lowest when the engine was running at part load, and quickly went up when it was running at full load. It was found that B20 fuel without additives had the highest HC of any fuel mix. This is explained by the poor combustion caused by the increased viscosity, less penetration and dispersion. When nanoparticles were added, a relatively low energy reaction allowed nano titanium to donate oxygen atoms. This occurred as a result of the catalytic action of  $\text{TiO}_2$  as stated in Eqs. (1)–(3). This indicates that titanium oxide contributed oxygen to the reduction of UHC, resulting in the production of titanium trioxide,  $\text{CO}_2$  and water [39].

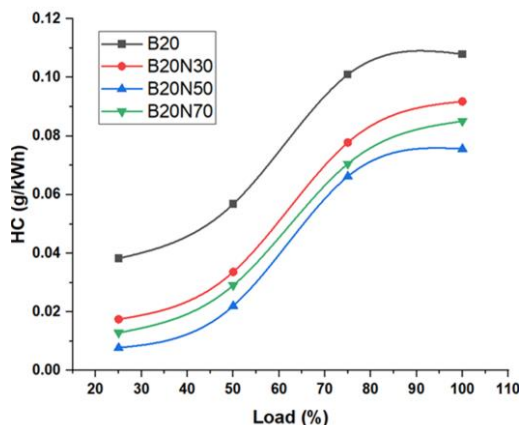


Fig. 9. Variations in HC emission for various fuel blends with respect to load.

Similar to the outcome previously reported by [40], diesel fuel HC was reduced by 7% when combined with  $\text{TiO}_2$  nanoparticles compared to pure diesel. The lowest HC was found in the particle size range of B20 + (10–30) nm (B20N30). Although 10 nm-sized nanoparticles offered a larger surface area, poor

dispersion must have resulted from the nanoparticles agglomeration and poor transport properties. Due to the nanoparticles inability to reach the areas where CO and HC creation were occurring, there was poor combustion and a modest rise in HC. According to the findings of this study, the B20N50 fuel composition was linked to the most substantial HC decrement of 35% when compared to B20 without any additives.

### 3.6.2. Carbon monoxide concentration

The lack of oxygen for the oxidation reaction is the primary cause of CO production. The full conversion of CO to  $\text{CO}_2$  is complicated when the temperature at which carbon is activated is high, as it usually is in diesel engine combustion [36]. However, because the activation temperature is higher, the conversion process takes longer.  $\text{TiO}_2$  serves as a catalyst and lowers the temperature when added to fuel. Consequently, the conversion of CO to  $\text{CO}_2$  can take place at low temperatures. This phenomenon might allow for a more thorough conversion of CO to  $\text{CO}_2$ , which would result in less CO. As shown in Fig. 10, B20 + (30–50) nm (B20N50) demonstrates the lowest CO value of the three nanoparticle doped fuel formulations, while B20 + (50–70) nm (B20N70) displays the highest. Nevertheless, these values were by 129.4% and 78.2% lower than the corresponding values for B20 without additives.

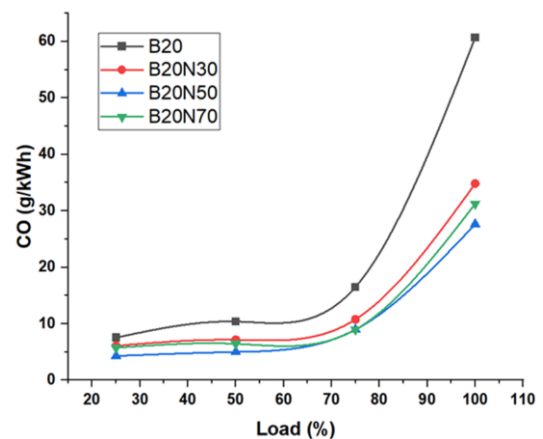


Fig. 10. Variations in CO emissions for various fuel blends with respect to load.

### 3.6.3. Smoke opacity findings

Unburned carbon molecules produced at the initial stage of combustion make up smoke. The main causes of smoke production are a lack of oxygen as well as the quenching action that takes place close to the cylinder wall. Carbon particles that function as a barrier to heat transfer are deposited at the wall surface as a result of quenching. As a result, the power output is reduced, frictional losses rise, and fuel consumption follows. The  $\text{TiO}_2$  nanoparticle addition has a significant catalytic impact on reducing the soot production. The addition of  $\text{TiO}_2$  lowers the carbon activation temperature to between  $200^\circ\text{C}$  and  $500^\circ\text{C}$ . Equation (3) demonstrates that this temperature mainly enhances the oxidation of soot particles to  $\text{CO}_2$ . As a result,  $\text{TiO}_2$  lessens the smoke production and emission. In conjunction with Pongamia

biodiesel [41], also it showed the decreased smoke opacity at 50 ppm and 100 ppm  $\text{TiO}_2$  nanoparticle concentrations. When the  $\text{TiO}_2$  nanoparticle amount was raised from 50 ppm to 100 ppm [42], an 8% decrease in smoke opacity was noticed. The fuel formulation with 30–50 nm-sized nanoparticles, or B20 + (30–50) nm (B20N50), exhibited the lowest soot emission of the three nanoparticle sizes taken into account in the current investigations (Fig. 11). The measured value for the operation of the B20 gasoline without additives was 53% greater than the observed value.

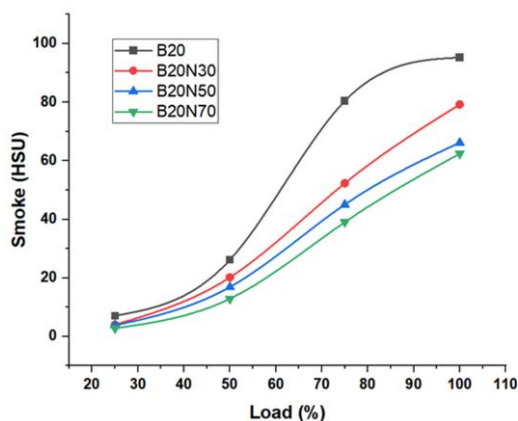


Fig. 11. Variations in smoke opacity emission for various fuel blends with respect to load.

### 3.6.4. The concentration of oxides of nitrogen

When utilized in diesel engines, biodiesel has a significant disadvantage in the emission of nitrogen oxides. Due to an abundance of oxygen, a hot combustion temperature, and a lengthy residence period,  $\text{NO}_x$  is formed. Fuel-borne oxygen encourages the oxidation of  $\text{N}_2$  during biodiesel combustion. The increased combustion temperature that is present in the combustion chamber further benefits this. There are several methods used to minimize  $\text{NO}_x$  in the emissions from tailpipes [43]. These methods, while lowering  $\text{NO}_x$ , also raise HC and CO levels or lower engine performance.

According to the findings shown in Fig. 12, combustion of the B20 without additives produced the largest  $\text{NO}_x$  emissions under all situations of load. B20 + (30–50) nm (B20N50) had the lowest  $\text{NO}_x$  value among the fuel formulations containing nanoparticles, which was 7.5% less than the comparable values observed for B20 + (10–30) nm (B20N30) and B20 + (50–70) nm (B20N70).

A unique method for decreasing  $\text{NO}_x$  and other emissions without sacrificing or even modestly boosting engine performance is to utilize  $\text{TiO}_2$  as a catalyst in engines. Equation (4), which describes how  $\text{TiO}_2$  first undergoes a reaction to generate  $\text{Ti}_2\text{O}_3$ , can be used to explain how  $\text{TiO}_2$  has a catalytic activity on  $\text{NO}_x$  reduction. By interacting with nitrogen oxides, this is further reduced to  $\text{TiO}_2$ , freeing nitrogen. Due to the greater activation energy of  $\text{N}_2$ ,  $\text{TiO}_2$  nanoparticles aid in lowering the temperature of the fuel-air mixture during this phase. The performance of diesel engines was also examined by Gracia and

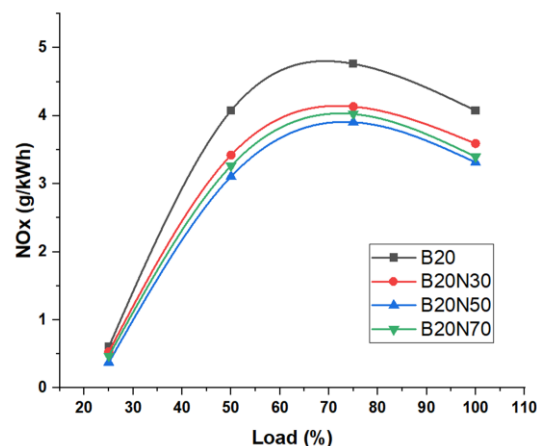


Fig. 12. Variations in  $\text{NO}_x$  emissions for various fuel blends with respect to load.

Rodreguaz [44] utilizing Pongamia biodiesel with  $\text{TiO}_2$  nanoparticles.  $\text{TiO}_2$ -doped esters showed lower  $\text{NO}_x$  values for all loads, according to the authors.

## 4. Conclusions

The engine characteristics of several B20-based fuel forms that contained  $\text{TiO}_2$  nanoparticles of different sizes were investigated through experiments. The research also used B20 which had no additives, for comparison. On the basis of the results, the following deductions and conclusions can be made:

- $\text{TiO}_2$  worked as a catalyst and significantly contributed to better engine combustion by raising BTE and lowering BSFC. The differences observed were significantly influenced by the nanoparticle size. The most notable reduction in BSEC by 6.4 %, when compared to the additive-free B20, was caused by nanoparticles smaller than 30 nm.
- The results showed that the B20+(30–50) nm (B20N50) fuel formulation was also linked to the highest rates of heat release and the highest pressures in the cylinders, the B20N30 blend has a heat release rate of 58.54 J/°CA and 72.3 bar, respectively, which is higher than that of the other blends and additive-free B20.
- By acting as a catalyst,  $\text{TiO}_2$  lowered the temperature at which carbon begins to oxidize, which aided in converting the HC, CO and soot to  $\text{CO}_2$  in the quenching regions of the combustion chamber and lowered engine exhaust emissions. Additionally, compared to other fuel formulations containing nanoparticles of different sizes or shapes, the B20 + (30–50) nm (B20N50) fuel formulation produced the least emissions. This result underlined the significance of the fuel nano additive size.

$\text{TiO}_2$  helped to decrease the  $\text{NO}_x$  at a relatively low level by assisting nitrogen oxides in oxidation-reduction processes and subsequently in their conversion to nitrogen. Once more, it was discovered that 30–50 nm-sized nano titanium were superior to their 10–30 nm and 50–70 nm-sized counterparts in terms of reducing  $\text{NO}_x$ .

## Acknowledgements

The research acknowledges the Renewable Energy and Alternatives Fuels Lab, Mechanical Engineering Department, National Institute of Technology Srinagar, India. The research was not supported by any other funding societies.

## References

- [1] Muradin, M. (2020). Environmental impact assessment of organic waste conversion technology for additives to liquid fuels. *Polityka Energetyczna - Energy Policy Journal*, 23(1), 135–150. doi: 10.33223/epj/118731
- [2] Agarwal, A.K. (2007). Biofuels (alcohols and biodiesel) applications as fuels for internal combustion engines. *Progress in energy and combustion science*, 33(3), 233–271. doi: 10.1016/j.peccs.2006.08.003
- [3] Dinesha, P., Kumar, S., & Rosen, M.A. (2019). Combined effects of water emulsion and diethyl ether additive on combustion performance and emissions of a compression ignition engine using biodiesel blends. *Energy*, 179, 928–937. doi: 10.1016/j.energy.2019.05.071
- [4] Wen, Z., & Petera, J. (2017). Numerical analysis of the effect of Hydrodynamics and operating conditions on biodiesel synthesis in a rotor-stator spinning disk reactor. *Chemical and Process Engineering*, 38(2), 265–281. doi: 10.1515/cpe-2017-0020
- [5] Wen, Z., & Petera, J. (2015). CFD numerical simulation of biodiesel synthesis in a spinning disc reactor. *Chemical and Process Engineering*, 36(1), 21–37. doi: 10.1515/cpe-2015-0002
- [6] Rakopoulos, C.D., Antonopoulos, K.A., Rakopoulos, D.C., Hountalas, D.T., & Giakoumis, E.G. (2006). Comparative performance and emissions study of a direct injection Diesel engine using blends of Diesel fuel with vegetable oils or biodiesels of various origins. *Energy Conversion and Management*, 47(18–19), 3272–3287. doi: 10.1016/j.enconman.2006.01.006
- [7] Sureshkumar, K., Velraj, R., & Ganesan R. (2008). Performance and exhaust emission characteristics of a CI engine fueled with Pongamia pinnata methyl ester (PPME) and its blends with diesel. *Renewable Energy*, 33(10), 2294–2302. doi: 10.1016/j.renene.2008.01.011
- [8] Muralidharan, K., Vasudevan, D., & Sheeba, K.N. (2011). Performance, emission and combustion characteristics of biodiesel fuelled variable compression ratio engine. *Energy*, 36(8), 5385–5393. doi: 10.1016/j.energy.2011.06.050
- [9] An, H., Yang, W.M., Maghbouli, A., Li, J., Chou, S.K., & Chua, K.J. (2013). Performance, combustion and emission characteristics of biodiesel derived from waste cooking oils. *Applied Energy*, 112, 493–499. doi: 10.1016/j.apenergy.2012.12.044
- [10] Agarwal, D., Kumar, L., & Agarwal, A.K. (2008). Performance evaluation of a vegetable oil fuelled compression ignition engine. *Renewable Energy*, 33(6), 1147–1156. doi: 10.1016/j.renene.2007.06.017
- [11] Alptekin, E. (2017). Emission, injection and combustion characteristics of biodiesel and oxygenated fuel blends in a common rail diesel engine. *Energy*, 119, 44–52. doi: 10.1016/j.energy.2016.12.069
- [12] Bertola, A., Li, R., & Boulouchos, K. (2003). Influence of Water-Diesel Fuel Emulsions and EGR on Combustion and Exhaust Emissions of Heavy Duty DI-Diesel Engines equipped with Common-Rail Injection System. *SAE Technical Paper*. doi: 10.4271/2003-01-3146
- [13] Qi, D.H., Geng, L.M., Chen, H., Bian, Y.Z., Liu, J., & Ren, X.C. (2009). Combustion and performance evaluation of a diesel engine fueled with biodiesel produced from soybean crude oil. *Renewable Energy*, 34(12), 2706–2713. doi: 10.1016/j.renene.2009.05.004
- [14] Izquierdo, J.F., Montiel, M., Palés, I., Outón, P.R., Galán, M., Jutglar, R., Villarrubia, M., Izquierdo, M., Hermo, M.P., & Ariz, X. (2012). Fuel additives from glycerol etherification with light olefins: State of the art. *Renewable and Sustainable Energy Reviews*. 16(9), 6717–6724. doi: 10.1016/j.rser.2012.08.005
- [15] Kumar, S., Dinesha, P., & Bran, I. (2019). Experimental investigation of the effects of nanoparticles as an additive in diesel and biodiesel fuelled engines: a review. *Biofuels*, 10(5), 615–622. doi: 10.1080/17597269.2017.1332294
- [16] E, J., Guanlin, L., Zhang Z., Han, D., Chen, J., Wei K., Gong J., & Yin, Z. (2019). Effect analysis on cold starting performance enhancement of a diesel engine fueled with biodiesel fuel based on an improved thermodynamic model. *Applied Energy*, 243, 321–335. doi: 10.1016/j.apenergy.2019.03.204
- [17] Kumar, S., Dinesha, P., & Bran, I. (2017). Influence of nanoparticles on the performance and emission characteristics of a biodiesel fuelled engine: An experimental analysis. *Energy*, 140, 98–105. doi: 10.1016/j.energy.2017.08.079
- [18] Prabu, A. (2018). Nanoparticles as additive in biodiesel on the working characteristics of a DI diesel engine. *Ain Shams Engineering Journal*, 9(4), 2343–2349. doi: 10.1016/j.asej.2017.04.004
- [19] Ramesh, D.K., Dhananjaya Kumar, J.L., Hemanth Kumar, S.G., Namith, V., Basappa Jambagi, P., & Sharath, S. (2018). Study on effects of Alumina nanoparticles as additive with Poultry litter biodiesel on Performance, Combustion and Emission characteristic of Diesel engine. *Materials Today Proceedings*, 5(1), 1114–1120. doi: 10.1016/j.matpr.2017.11.190
- [20] D'Silva, R., Fernandes, N., Menezes, M., D'Souza P., Pinto, V., Kaliveer, V., Gopalakrishna, B.K., & Bhat, T. (2019). Effect of TiO<sub>2</sub> nanoparticle concentration in Pongamia Pinnata methyl ester on performance and emission characteristics of CI engine. *AIP Conference Proceedings*, 2080(1). doi: 10.1063/1.5092909
- [21] Mitchell, M.R., Link, R.E., Kao, M.J., Ting, C.C., Lin, B.F., & Tsung, T. T. (2008). Aqueous aluminum nanofluid combustion in diesel fuel. *Journal of Testing and Evaluation*, 36(2), 186–190. doi: 10.1520/JTE100579
- [22] Xin, Z., Tang, Y., Man, C., Zhao, Y., & Ren, J. (2013). Research on the impact of CeO<sub>2</sub>-based solid solution metal oxide on combustion performance of diesel engine and emissions. *Journal of Marine Science and Application*, 12, 374–379. doi: 10.1007/s11804-013-1197-7
- [23] Kumar, S., Dinesha, P., & A. Rosen, M. (2019). Effect of injection pressure on the combustion, performance and emission characteristics of a biodiesel engine with cerium oxide nanoparticle additive. *Energy*, 185, 1163–1173. doi: 10.1016/j.energy.2019.07.124
- [24] Sajith, V., Sobhan, C.B., & Peterson, G.P. (2010). Experimental investigations on the effects of cerium oxide nanoparticle fuel additives on biodiesel. *Advances in Mechanical Engineering*, 2. doi: 10.1155/2010/581407
- [25] Mirzajanzadeh, M., Tabatabaei, M., Ardjmand, M., Rashidi, A., Ghobadian, B., Barkhi, M., & Pazouki, M. (2015). A novel soluble nano-catalysts in diesel-biodiesel fuel blends to improve diesel engines performance and reduce exhaust emissions. *Fuel*, 139, 374–382. doi: 10.1016/j.fuel.2014.09.008
- [26] Selvan, V.A.M., Anand, R.B., & Udayakumar, M. (2009) Effects of cerium oxide nanoparticle addition in diesel and diesel-biodiesel-ethanol blends on the performance and emission characteristics of a CI engine. *ARPJ Journal of Engineering and Applied Sciences*, 4(7), 1–6.
- [27] Ahmed, M.M., Pali, H.S., & Khan, M.M. (2022). Experimental analysis of diesel/biodiesel blends with a nano additive for the performance and emission characteristics of CI Engine. *International Journal of Engine Research*, 24(11), 4500–4508. doi: 10.1177/14680874221132958
- [28] Pali, H.S., Kumar, N., & Alhassan, Y. (2015). Performance and emission characteristics of an agricultural diesel engine fueled with blends of Sal methyl esters and diesel. *Energy Conversion and Management*, 90, 146–153. doi: 10.1016/j.enconman.

- 2014.10.064
- [29] Hosseini, S.H., Taghizadeh-Alisaraei, A., Ghobadian, B., & Abbaszadeh-Mayvan, A. (2017). Effect of added alumina as nano-catalyst to diesel-biodiesel blends on performance and emission characteristics of CI engine. *Energy*, 124, 543–552. doi: 10.1016/j.energy.2017.02.109
- [30] Karthikeyan, S., Elango, A., & Prathima, A. (2016). The effect of cerium oxide additive on the performance and emission characteristics of a CI engine operated with rice bran biodiesel and its blends. *International Journal of Green Energy*, 13(3), 267–273. doi: 10.1080/15435075.2014.952419
- [31] Reddy, S.N K., & Wani, M.M. (2020). A comprehensive review on effects of nanoparticles-antioxidant additives-biodiesel blends on performance and emissions of diesel engine. *Applied Science and Engineering Progress*, 13(4), 285–298. doi: 10.14416/J.ASEP.2020.06.002
- [32] Sharma, A., Pali, H.S., Kumar, M., Singh, N.K., Singh, Y., & Singh, D. (2022). Study the effect of optimized input parameters on a CRDI diesel engine running with waste frying oil methyl ester-diesel blend fuel with ZnO nanoparticles: a response surface methodology approach. *Biomass Conversion and Biorefinery*, 13, 13127–13152. doi: 10.1007/S13399-021-02158-6
- [33] Gürü, M., Koca, A., Can, Ö., Çinar, C., & Şahin, F. (2010). Biodiesel production from waste chicken fat based sources and evaluation with Mg based additive in a diesel engine. *Renewable Energy*, 35(3), 637–643. doi: 10.1016/j.renene.2009.08.011
- [34] Bednarski, M., Orliński, P., Wojs, M., & Gis, M. (2020). Evaluation of the heat release rate during the combustion process in the diesel engine chamber powered with fuel from renewable energy sources. *Bulletin of the Polish Academy of Sciences, Technical. Sciences*, 68(6), 1333–1339. doi: 10.24425/bpasts.2020.135394
- [35] Pan, W., Yao, C., Han, G., Wei, H., & Wang, Q. (2015). The impact of intake air temperature on performance and exhaust emissions of a diesel methanol dual fuel engine. *Fuel*, 162, 101–110. doi: 10.1016/j.fuel.2015.08.073
- [36] Hussain Vali, R., Hoang, A.T., Wani, M.M., Pali H.S., Balasubramanian, D., Arici, M., Said, Z., & Nguyen, X.P. (2022). Optimization of variable compression ratio diesel engine fueled with Zinc oxide nanoparticles and biodiesel emulsion using response surface methodology. *Fuel*, 323, 124290. doi: 10.1016/j.fuel.2022.124290
- [37] Pali, H.S., Sharma, A., Kumar, M., Annakodi, V.A., Nguyen, V.N., Singh, N.K., Singh, Y., Balasubramanian, D., Deepan-raj, B., Truong T.H., & Nguyen, P.Q.P. (2023) Enhancement of combustion characteristics of waste cooking oil biodiesel using TiO<sub>2</sub> nanofluid blends through RSM. *Fuel*, 331(part 1). doi: 10.1016/j.fuel.2022.125681
- [38] Logothetidis, S., Patsalas, P., & Charitidis, C. (2003). Enhanced catalytic activity of nanostructured cerium oxide films. *Materials Science and Engineering: C*, 23(6–8), 803–806. doi: 10.1016/j.msec.2003.09.081
- [39] Mei, D., Li, X., Wu, Q., & Sun, P. (2016). Role of Cerium Oxide Nanoparticles as Diesel Additives in Combustion Efficiency Improvements and Emission Reduction. *Journal of Energy Engineering*, 142(4), 1–6. doi: 10.1061/(asce)jey.1943-7897.0000329
- [40] Shaisundaram, V.S., Chandrasekaran, M., Mohan Raj, S., & Muraliraja, R. (2020). Investigation on the effect of thermal barrier coating at different dosing levels of cerium oxide nanoparticle fuel on diesel in a CI engine. *Intenational Journal of Ambient Energy*, 41(1), 98–104. doi: 10.1080/01430750.2018.1451385
- [41] Appavu, P., & Ramanan, M.V. (2020). “Study of emission characteristics of a diesel engine using cerium oxide nanoparticle blended pongamia methyl ester. *International Journal of Ambient Energy*, 41(5), 524–527. doi: 10.1080/01430750.2018.1477063
- [42] Seela, C.R., Sankar, B.R., Kishore, D., & Babu, M.V.S. (2019). Experimental analysis on a DI diesel engine with cerium-oxide-added Mahua methyl ester blends. *International Journal of Ambient Energy*, 40(1), 49–53. doi: 10.1080/01430750.2017.1360203
- [43] Singh, Y., Pali, H.S., Singh, N.K., Sharma, A., & Singla, A. (2022). Effect of nanoparticles as additives to the biofuels and their feasibility assessment on the engine performance and emission analysis - A review. *Proceeding of the Institution of Mechanical Engineers, Part E: Journal of Process Mechanical Engineering*, 237(2). doi: 10.1177/09544089221109723
- [44] Fernández-García, M., & Rodríguez, J.A. (2011). Metal Oxide Nanoparticles. In: *Encyclopedia of Inorganic and Bioinorganic Chemistry*. Chichester, UK, John Wiley & Sons, Ltd; eibc0331. doi: 10.1002/9781119951438.eibc0331